EPJ Web of Conferences **302**, 05003 (2024) https://doi.org/10.1051/epjconf/202430205003
SNA + MC 2024

New simulation controls for the molten salt reactors related neutronic evolution code REM

Louiliam Clot[1,2,*], *Elsa* Merle[1], *Axel* Laureau[1], *Daniel* Heuer[1], *Léa* Tillard[2], and *Gérald* Senentz[2]

[1]LPSC, IN2P3/CNRS, Grenoble INP - UGA, Univ. Grenoble Alpes, 53 Avenue des Martyrs, 38026 Grenoble, France
[2]Orano, 125 Avenue de Paris, 92320 Châtillon, France

Abstract. The in-house precision-driven material evolution code REM has been developed since the early 2000s at CNRS/LPSC Grenoble for the study and optimisation of molten salt reactors (MSR). In recent years, a particular family of these reactors has been of great interest to many players in the industry, such as the Orano group: MSRs operated as plutonium and minor actinide converters. Depletion simulation purposes has led to the development of new methods for managing supplies and the addition of new constraint parameters to the REM code. These new developments have made it possible to add new physico-chemical constraints of interest in the study of burner MSRs, such as control of the alkali or alkaline-earth fraction, or control of the volume by constraining the supply or by adding a dynamic expansion tank. These new perspectives have led to work on the numerical stabilisation of the system and the especially supplies, which has smoothed out some reactor characteristics and opened the way to interesting new research possibilities. Finally, chemical considerations on the valency of the elements and the electroneutrality of the salt raise questions about the different feeding strategies to be studied and could lead to the development of a new model for extracting materials.

1 Introduction

Molten salt reactors (MSRs), innovative reactors where the fuel is a liquid circulating molten salt that acts also as coolant, have been studied at CNRS since the early 2000s and are of growing interest for the conversion and incineration of plutonium and minor actinides produced for example in pressurised water reactors.
The diversity of MSR concepts gives this family of reactors great versatility. The choice of the fuel salt (based on LiF for the fluoride versions or on NaCl for the chloride ones), of the neutron spectrum (from thermal to fast spectrum), the size and power allow the development of large breeder reactors as well as small burner AMRs (Advanced Modular Reactor).
The aim of this paper is to present the new developments made in the REM code from 2023 onwards to improve the management of supplies in burner MSRs and to better simulate the physical aspects inherent to this type of reactor. Section 2 presents the principle of neutronic evolution codes and details the former algorithm of the REM code. The new developments

*e-mail: louiliam.clot@lpsc.in2p3.fr

carried out in the REM code are detailed in section 3, while the new constraints and associated evolution strategies are explained in section 4.

2 Depletion simulations and the REM code

2.1 Depletion simulations

The depletion simulations couple the static resolution of the neutron transport equation, solved in this work with a Monte-Carlo (MC) code, with an evolution module that solves the Bateman equations between two neutron transport steps. Figure 1 shows the operating principle of the SMURE code [1], which can be generalised to all evolution codes. Once the

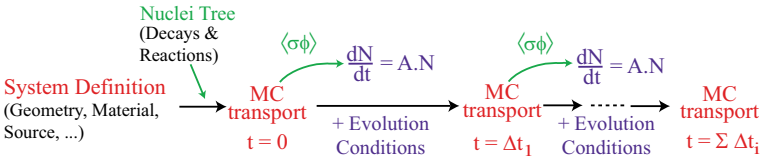

Figure 1. Principle of neutronic evolution calculation [1]

main parameters of the system under consideration and the nuclear data have been defined, an initial Monte-Carlo calculation is carried out to calculate the reactivity and neutron flux at reactor start-up. These data are used to solve the Bateman equations (1), during which certain conditions can be applied to control the evolution, such as setting the reactor power and/or the reactivity constant. Solving the Bateman equations will update the materials N_i to perform a static Monte-Carlo calculation again and so on until the end of the evolution.

$$\frac{\mathrm{d}N_i}{\mathrm{d}t} = \sum_{j\neq i}\langle\sigma_{j\to i}\phi\rangle N_j - \sum_{j\neq i}\langle\sigma_{i\to j}\phi\rangle N_i + \sum_{j\neq i}\lambda_{j\to i}N_j - \lambda_i N_i = \sum A_{ij}N_j \tag{1}$$

For Molten salt reactors neutronics simulation, adaptation of the algorithm are needed. Equation (1) is established for the evolution of a core with no material addition or extraction during evolution, which is suitable for most studies and systems. For the MSR concepts based on continuous material supply and extraction during reactor operation, it is necessary to include additional terms to the Bateman equations. These terms are presented in equation (2) [2]. Continuous processing is simulated with a time constant $\lambda_i^{\text{processing}}$ (which is, for example, 30 seconds for the extraction of gaseous fission products), while the supply is represented by a flow rate S_i.

$$\frac{\mathrm{d}N_i}{\mathrm{d}t} = \sum A_{ij}N_j - \lambda_i^{\text{processing}}N_i + S_i \tag{2}$$

2.2 The REM code

2.2.1 Overview

The in-house REM code has been developed since the early 2000s at CNRS/LPSC Grenoble [2, 3]. The code simulates the evolution of materials under controls using the MCNP Monte-Carlo code [4] to solve the neutron transport and a Runge-Kunta 4 (RK4) algorithm for an evolution driven by precision. This code has been designed to be natively adapted for continuous loading reactors such as CANDUs and MSRs and has been tested and compared with other similar codes, notably as part of the European EVOL project [5]. Other codes have been developed since then such as MOSARELA [6], SMURE [1, 7] and OpenMC [8].

2.2.2 Algorithm principle

The first step of the calculation consists of the definition of geometries, cells, materials and all the control and evolution settings and ranges for supplies.
Then, during the code processing, there are different scales of calculation steps from:

- "Integration steps" where the MSR related Bateman's equation (2) is solved with a RK4 integration algorithm using variable steps;
- "Adjustment steps" where supplies S_i are updated inside Bateman's equation;
- "Control cycles" that manage adjustment steps for all supplies;
- "Neutron transport steps" where static transport calculations are performed to update reaction rates.

Adjustment steps and control cycles

In the REM code, the supplies are continuous while in most depletion codes, MSRs are supplied per batchs. The flow rate F_k of each supply S_k is adjusted during the integration process at each adjustment step according to a constraint parameter C_k and its target value C_k^{target}. The physical parameters included in the code are as follows:

- Reactivity k_{eff};
- Proportion of heavy nuclei f_{HN} ($Z \geq 89$) in the salt;
- Proportion of heavy nuclei plus magnesium f_{AnMg} ($Z = 12$) in the salt;
- Proportion of transuranium elements f_{TRU} ($Z \geq 93$) in the salt;
- Proportion of a specific element f_Z in the salt.

Each S_k is supplied in a cell to keep C_k at C_k^{target}.
The reference MSFR is a breeder reactor using the ^{232}Th/^{233}U cycle with a LiF−(HN)F_4 salt and maintaining the fraction of heavy nuclei at 22.5% corresponding to the lowest melting point eutectic, optimised in particular as part of the European EVOL project [5]. A more complete description of this concept can be found in [2, 5]. In the REM simulation of this reactor, there are three supplies correlated with three contraints:

- ^{233}U supplied into the core to keep the reactivity at −170 pcm, which corresponds to prompt criticality, taking into account the circulation of precursors in the salt [9];
- ^{232}Th supplied into the core to keep the proportion of heavy nuclei at 22.5%;
- ^{232}Th supplied into the fertile blanket to keep the proportion of heavy nuclei at 22.5%.

Reactivity is impacted both by the supply of ^{233}U and by the breeding of ^{232}Th which guarantees a constant fraction of heavy nuclei.
Each constraint C_k variation depends on the time t and the variation of supply flow rate F_k according to equation (3).

$$\Delta C_k = \frac{\partial C_k}{\partial t}\Delta t + \frac{\partial C_k}{\partial F_k}\Delta F_k \tag{3}$$

So the variation in supply flow rate depends on the time and the variation in constraint according to equation (4).

$$\Delta F_k = \frac{\partial F_k}{\partial C_k}\left(\Delta C_k - \frac{\partial C_k}{\partial t}\Delta t\right) \tag{4}$$

To calculate the variation in supply flow rate ΔF_k, each control cycle is subdivided into two adjustment steps:

- The first step is done without changing the supply variation to obtain the derivative $\frac{\partial C_k}{\partial t} = \frac{\Delta C_k}{\Delta t}$;
- The second step is used to calculate the value of $\frac{\partial F_k}{\partial C_k}$. To do this, the code will approximate the derivative $\frac{\partial C_k}{\partial t}$ with the sliding average of the last ℓ values to smooth evolution and use formula (3) to calculate the last ℓ deviations from the target. In this way, the derivative $\frac{\partial F_k}{\partial C_k}$ is calculated as shown in formula (5).

$$\frac{\partial F_k}{\partial C_k} = \frac{\sum_{\ell \text{ last}} \frac{\Delta F_k}{C_k^{\text{target}} - C_k - \frac{\partial C_k}{\partial t}\Delta t}}{\ell} \tag{5}$$

Once the two derivatives have been calculated, the supply flow rate is adjusted using the formula (4) and the code moves on to the next supply in another control cycle.

Neutron transport / MCNP steps

Figure 2 shows the structure of the calculation and the organization between MCNP steps (rectangles with MCNP_k inside) and evolution steps (dashed arrows between t_k and t_{k+1}) from the beginning to time t_2. Each MCNP step k has a dynamic length Δt_k adjusted as follows:

- Starting from t_k, a first evolution is performed to $t_{k+1} = t_k + \Delta t_k$ using $\langle \sigma\phi \rangle_k$. At this time, REM knows the proportions N_i at t_{k+1}.
- Transport is solved by running MCNP_{k+1} which gives the updated $\langle \sigma\phi \rangle_{k+1}$.
- Back to t_k, a second evolution is performed to t_{k+1} with an interpolation f between $\langle \sigma\phi \rangle_k$ and $\langle \sigma\phi \rangle_{k+1}$. The interpolation can be a ramp, a slope or the mean of the two values. This evolution gives the proportions N'_i at t_{k+1}.
- A χ^2 test is performed between proportions N_i and N'_i as shown in equation (6). The weights w_i are set to 1 by default and are currently set to 0 for the isotopes present in the supplies. The absolute_precision_coefficient is given in the initial setup of the REM code as parameters χ^2_{min} and χ^2_{max} used as follows :
  - If $\chi^2 > \chi^2_{\text{max}}$ then another MCNP'_{k+1} is launched to re-update reaction rates and performed a third evolution between t_k and t_{k+1} to obtain proportions N''_i. Then another χ^2 test is performed to compare N'_i and N''_i
  - If the test is still unsatisfactory then the length of the next step is reduced : $\Delta t_{k+1} = \Delta t_k \,/\, \sqrt{2}$
  - If $\chi^2 < \chi^2_{\text{min}}$ and if the length of the previous step has not been reduced then the lenght of the next step is increased : $\Delta t_{k+1} = \Delta t_k \times \sqrt{2}$
  - Else, the next step has the same length and $\Delta t_{k+1} = \Delta t_k$

$$\chi^2 = \sqrt{\sum_{\text{cells}} \frac{\sum_{i=1}^{n_{\text{isotopes}}} w_i (N'_i - N_i)^2}{\left(\sum_{i=1}^{n_{\text{isotopes}}} N_i \right)^2}} \Bigg/ \text{absolute\_precision\_coefficient} \tag{6}$$

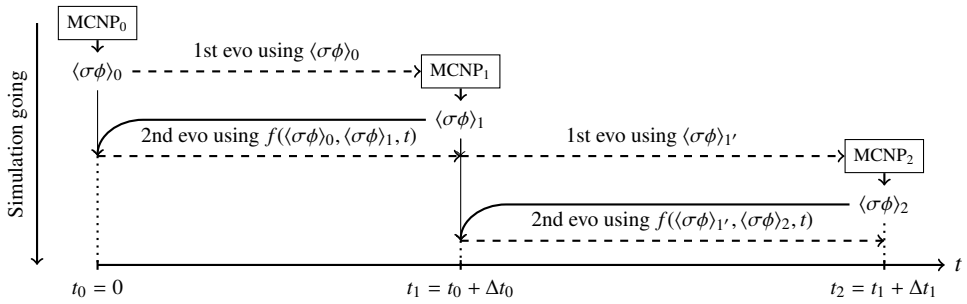

Figure 2. Principle of the organisation between MCNP steps and evolution steps in the REM code

2.3 Model limitations

As part of a collaboration between CNRS/LPSC Grenoble and Orano [7, 10], studies on burner MSRs have begun and have revealed certain limitations of the exiting model. Three main and correlated limitations have been identified:

1. Limitation on the types of constraints available as some seemed to be missing to carry out some studies;

2. To compensate the degradation of the isotopic fissile quality of their fuel, the fuel salt volume of burner reactors tends to increase, exceeding the physical volume of the core constrained by the geometry. Plus, the addition of new constraints - and therefore new supplies - tends to amplify this phenomenon, except of course for the constant ionic volume constraint (see section 4.1).

3. Finally, the multiplication of constraints and supplies tends to make the model unstable.

This led to new developments in the REM code, including the implementation of new constraints and a dynamic expansion tank to manage excess salt (section 4) and a new method of adjustment for the supplies (see section 3 below).

3 New numerical developments

3.1 New algorithm implementation

The new adjustment strategy adopted for the REM code is to consider all the supplies at each control cycle. To do this, the n equations (3) - with n number of supplies - are thought of as a single vector equation (7) with $\bar{\mathbf{J}}_{\mathbf{C}}(\mathbf{F})$ the Jacobian matrix of the system defined by formula (8), $\mathbf{F}$ the flow rate vector and $\mathbf{C}(\mathbf{F})$ the associated constraints vector. Now all the constraints depend on all the supplies, while the old algorithm acted as if the Jacobian matrix were diagonal.

$$\Delta\mathbf{C}(\mathbf{F}) = \frac{\partial\mathbf{C}(\mathbf{F})}{\partial t}\Delta t + \bar{\mathbf{J}}_{\mathbf{C}}(\mathbf{F})\,\Delta\mathbf{F} \tag{7}$$

$$\bar{\mathbf{J}}_{\mathbf{C}}(\mathbf{F}) = \begin{bmatrix} \frac{\partial C_1(\mathbf{F})}{\partial F_1} & \cdots & \frac{\partial C_1(\mathbf{F})}{\partial F_n} \\ \vdots & \ddots & \vdots \\ \frac{\partial C_n(\mathbf{F})}{\partial F_1} & \cdots & \frac{\partial C_n(\mathbf{F})}{\partial F_n} \end{bmatrix} \tag{8}$$

So equations (4) become now equation (9).

$$\Delta\mathbf{F} = \bar{\mathbf{J}}_{\mathbf{C}}^{-1}(\mathbf{F})\left(\mathbf{C}^{\text{target}} - \mathbf{C}(\mathbf{F}) - \frac{\partial\mathbf{C}(\mathbf{F})}{\partial t}\Delta t\right) \tag{9}$$

Each control cycle comprises $2(n+1)$ adjustment steps. The odd steps are used to calculate the derivatives forming the columns of the Jacobian matrix by modifying a supply and looking at the impact of this change on all the constraints. The even steps are used to calculate the time derivatives without adjusting the supplies ($\Delta\mathbf{F} = \mathbf{0}$) to finally take their average over the cycle to calculate formula (9). Figure 3 shows the chlorine supply in a simulation with three supplies: NaCl, $MgCl_2$ and $PuCl_3$, the chlorine supply being a condensed image of these three supplies. The control cycles are shown in red and the adjustment steps in blue. Each change in chlorine flow rate corresponds to an adjustment step and once the $8 = 2(3+1)$ steps have been completed, all the supplies are updated at the same time and a new control cycle begins.

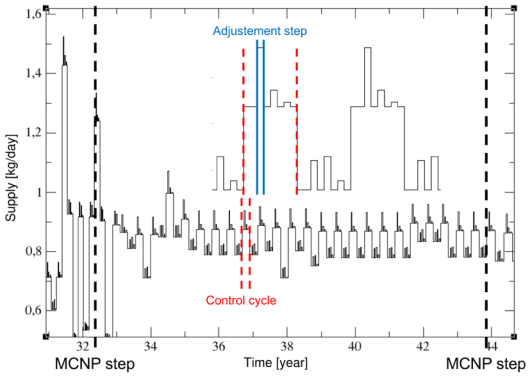

Figure 3. Details of the different steps during an MCNP step on a chlorine supply

3.2 Preliminary results on the EVOL MSFR case

Figures 4 and 5 show the in-core uranium supply (flow rate and cumulative) and Figure 6 shows the reactivity in the MSFR core during an evolution, with the old controls as implemented at the beginning of 2023 (in black) and with the new controls (in red).

Despite the radically different altitudes of the two supply curves (Figure 4 left), the supplies are equivalent on average, as shown in Figure 4 right, where the cumulative supplies only deviate by 2% after 200 years (from 22,419 to 21,974 kg).

The new method of adjusting the supplies has tended to stabilise them out compared with the old method. Figure 5 on the left shows that the new supplies have a continuous character that the old ones did not have. This can be seen clearly in Figure 5 right, where the new cumulative supply is smoother than the old one, which is crenellated. Finally, it is possible to see in Figure 5 left small peaks on the new supply: these are the small changes used to calculate the derivatives of the column of the Jacobian matrix as illustrated in Figure 3. By way of illustration, formula (10) shows the numerical value of the Jacobian matrix during a control cycle at the end of the evolution, showing that the approximation made by the old adjustment model that this matrix was diagonal is not correct in this case.

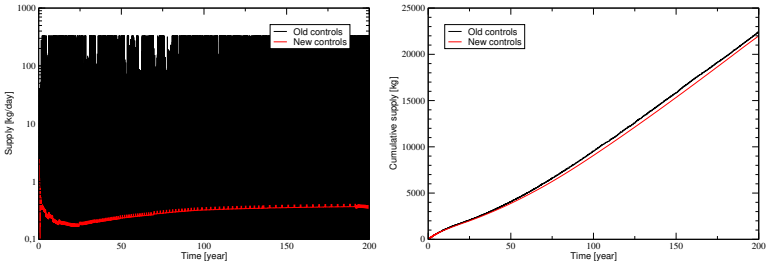

Figure 4. Supply (left) and cumulative supply (right) of ^{233}U in the MSFR during 200 years of evolution

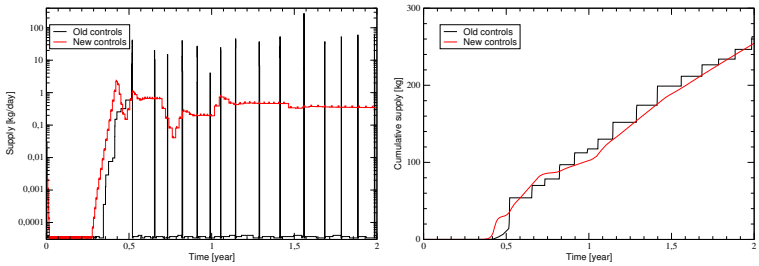

Figure 5. Supply (left) and cumulative supply (right) of ^{233}U in the MSFR during 2 years of evolution

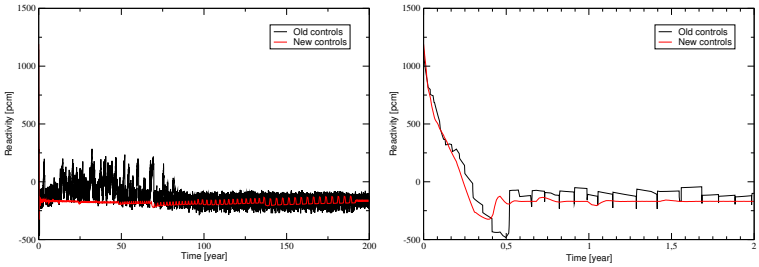

Figure 6. Reactivity in the MSFR core during 200 years (left) and 2 years (right) of evolution

$$\bar{\mathbf{J}}_{\mathbf{C}}(\mathbf{F}) = \begin{bmatrix} 56.91439 & -6.272225 & -1.242452 \\ 2.383977 \times 10^{-5} & 2.405735 \times 10^{-5} & -2.301743 \times 10^{-9} \\ -1.868511 \times 10^{-9} & -1.080081 \times 10^{-10} & 5.915808 \times 10^{-5} \end{bmatrix} \tag{10}$$

Making the supplies more stable has positive effects on the constraints they control, as illustrated in Figure 6, which shows that core reactivity oscillates much less around its target value and is slightly more responsive.

3.3 Dynamic expansion tank implementation

In addition to developing new controls, the ability to dynamically modify the geometry of a core cell - known as the expansion tank - have been implemented. This process takes place at each MCNP step: when the parameter is activated, the REM code calculates the ionic volume

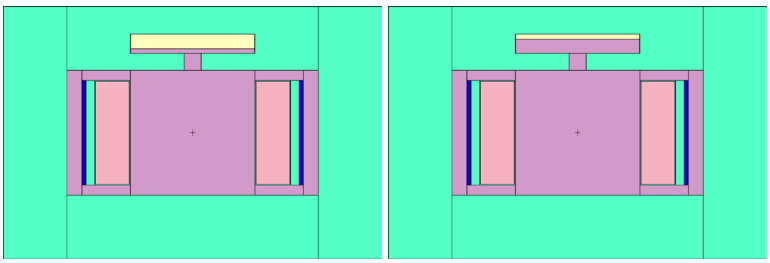

Figure 7. MCNP visualisation of Cl-MSFR [11] geometry at the beginning of the evolution (left) and after 50 years (right)

of the fuel salt and adjusts the height of the vessel to match the geometric volume when the transport is solved. Figure 7 shows two visualisations of the geometry of the Cl-MSFR concept developed by Hugo Pitois in his PhD thesis [11] at two instants of an evolution. The fuel salt is in purple, the fertile blanket is in pink, the B_4C neutron protection is in blue, the steel reflectors are in green and the argon sky in the empty part of the tank is in yellow. As the volume of fuel salt increased during evolution, the height of the salt level in the vessel increased accordingly.

4 New physical models

4.1 Implementation of new constraints

As mentioned in section 2.3, new constraints have been added to the REM code:

- Proportion of alkali metals f_A in the salt;
- Proportion of alkaline earth metals f_{AT} in the salt;
- Proportion of alkali and alkaline earth metals f_{AAT} in the salt;
- Constant ionic volume V of the salt;
- Electroneutrality of the salt.

The implementation of these new constraints was motivated by new considerations in fuel salt chemistry. For example, taking into consideration the ternary salt $NaCl–MgCl_2–PuCl_3$, the proportions of alkali and alkaline-earth will make it possible to control the position of the composition on the ternary, in particular to remain close to the eutectic minimum melting temperature of the salt. Controlling the constant volume ensures that the feeds are equivalent in volume to the extractions and could eliminate the need for a dynamic expansion tank. Finally, the aim of controlling the electroneutrality of the salt is to match the theoretical valencies of the elements in the salt with those of the halogens. Formula (11) shows the result of the fission of a plutonium nucleus into two fission products FP^1 and FP^2 with the distribution of the three initial chlorine atoms. If the sum of the valencies of the two fission products is not equal to 3, then the resulting lack or excess of chlorine can influence the reducing or oxidising nature of the salt, which has a direct impact on its corrosive nature on structural materials. To this end, the theoretical valency values of all the elements (positive for cations and negative for anions) have been statically implemented in the code to measure any discrepancies, which could lead to further studies to update them.

$$PuCl_3 \longrightarrow (FP^1)Cl_x + (FP^2)Cl_{3-x} \tag{11}$$

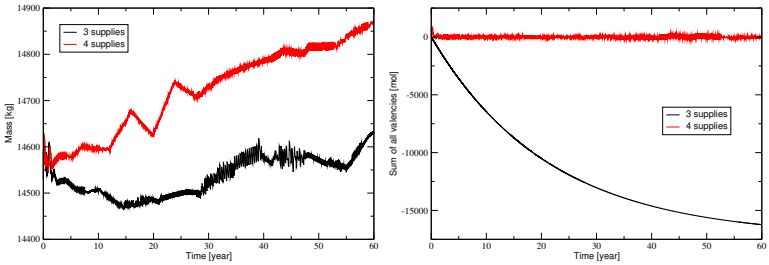

Figure 8. Mass of total salt (left) and valency of salt elements (right)

4.2 New strategies for the evolution simuations

The physico-chemical problems raised another question about the supplying strategy to adopt. Again with regard to a ternary salt NaCl−$MgCl_2$−$PuCl_3$, it is possible to consider either supplying in elements (Na, Mg, Pu and Cl) or supplying in species (NaCl, $MgCl_2$ and $PuCl_3$). Both strategies have their benefits and drawbacks. Figure 8 shows the total salt mass and the sum of the valences of the salt elements for a simulation of a burner MSR with three supplies (in black) or four supplies (in red). In these simulations, a fraction of all the fuel salt is continuously extracted without reinjecting any material.

4.2.1 Three supplies strategy

The simulation using three supplies is the most "physically realistic" strategy, since it simulates a supply in salts rather than element by element, which is of interest in the study of deployment scenarios of such reactors. It requires three correlated constraints. The first obvious constraint is reactivity control, provided by the $PuCl_3$ supply. The second constraint used is the control of the alkali fraction to keep the proportion of NaCl in the salt constant, by supplying NaCl. Finally, the third $MgCl_2$ supply is designed to keep the volume of salt constant to compensate for the volume extracted continuously. Figure 8 on the right shows that this strategy causes an excess of chlorine (because chlorine has a negative valency), which would make the salt very oxidising in a real physical reactor: in reality, the elements would spontaneously change valency to match the right number of chlorine atoms. The lack of experiments and data means that it is not possible to make this model "more physical" without making too many assumptions at the moment.

4.2.2 Four supplies strategy

To solve this problem, the elements can be separated to add a chlorine supply. So, in addition to the constraints of reactivity (coupled with the plutonium supply), alkali fractions in the salt (with a sodium supply) and constant volume with a magnesium supply, we need to add the electronegativity constraint, which will be controlled by the chlorine supply. Figure 8 right shows that the valency remains close to 0 but Figure 8 left shows that the total mass of salt is larger with this strategy, mainly because the amount of sodium and magnesium is higher than in the 3 supplies strategy to match the excessive amounts of chlorine. This strategy respects electroneutrality - modulo the assumptions made about the valences of the elements - but could overestimate the mass balances.

5 Conclusions and perspectives

A new constraint-driven supply management model has been implemented in the REM code. This model improves the algorithm by stabilising the supplies, without fundamentally changing the material balances compared with the previous model. This new stability makes it possible to add new constraints, which is of interest in the study of all kinds of MSRs including burner concepts in order to comply with their specific physical as well as chemical constraints, such as the fraction of certain families of elements (alkalis and alkaline earths), the control and matching of volume (by controlling the supply or adding a dynamic expansion vessel) and the management of the electroneutrality of the salt by controlling the valences of the elements.
These new controls and the flexibility they provide pave the way for new questions on the supply strategies to be adopted to comply with assumptions and constraints linked to physics, chemistry or scenarios. Finally, as a mirror image of the work carried out on supplies, studies on a new management of extractions and processing may be necessary, possibly by working on equivalence models.

References

[1] O. Méplan *et al*, MURE v.3 : SMURE, Serpent-MCNP Utility for reactor Evolution, *User Guide - 2nd Edition*, LPSC 17002 (2021)

[2] X. Doligez *et al*, *Coupled study of the Molten Salt Fast Reactor core physics and its associated reprocessing unit*, Annals of Nuclear Energy **64**, 430440 (2014)

[3] E. Merle-Lucotte, D. Heuer, M. Allibert, X. Doligez, V. Ghetta, *Simulation Tools and New Developments of the Molten Salt Fast Reactor*, Contribution A0115, Proceedings of European Nuclear Conference ENC2010, Barcelone, Spain (2010)

[4] X-5 Monte Carlo Team, *General Monte Carlo N-Particle Transport Code*, Version 5, LA-UR-03-1987, Los Alamos National Laboratory (2003)

[5] M. Brovchenko, J.-L. Kloosterman, L. Luzzi, E. Merle, D. Heuer *et al*, *Neutronic benchmark of the molten salt fast reactor in the frame of the EVOL and MARS collaborative projects*, EPJ Nuclear Sci. Technol. **5** (2019)

[6] P.-E. Dufour *et al*, *A tool to estimate isotopic evolution for actinides transmutation dedicated fast molten salt reactors*, Proceedings of the International Conference SFM 2024, Vienna, Austria (2024)

[7] L. Clot, *Modélisation du recyclage des matières dans les réacteurs à sels fondus*, Master 2 intership report, Grenoble INP - Phelma, UGA, Grenoble, France (2022)

[8] Paul K. Romano, Nicholas E. Horelik, Bryan R. Herman, Adam G. Nelson, Benoit Forget, and Kord Smith, *OpenMC: A State-of-the-Art Monte Carlo Code for Research and Development*, Ann. Nucl. Energy, **82**, 90–97 (2015).

[9] A. Laureau, M. Aufiero, P. Rubiolo, E. Merle-Lucotte, D. Heuer, *Transient Fission Matrix: kinetic calculation and kinetic parameters β_{eff} and Λ_{eff} calculation*, Annals of Nuclear Energy, **85**, p. 10351044 (2015)

[10] L. Mesthiviers, *Transuranic elements burning efficiency in Molten Salt Reactors (MSR)*, PhD Thesis, Université Grenoble Alpes, Grenoble, France (2022)

[11] H. Pitois, *Design and optimisation of a Molten Salt Fast Reactor using chloride salts and uranium cycle*, PhD Thesis, Université Grenoble Alpes, Grenoble, France (2023)